



## The Distribution of Stress and Velocity in Glaciers and Ice-Sheets

J. F. Nye

*Proceedings of the Royal Society of London. Series A, Mathematical and Physical Sciences*, Vol. 239, No. 1216. (Feb. 12, 1957), pp. 113-133.

Stable URL:

<http://links.jstor.org/sici?sici=0080-4630%2819570212%29239%3A1216%3C113%3ATDOSAV%3E2.0.CO%3B2-X>

*Proceedings of the Royal Society of London. Series A, Mathematical and Physical Sciences* is currently published by The Royal Society.

---

Your use of the JSTOR archive indicates your acceptance of JSTOR's Terms and Conditions of Use, available at <http://www.jstor.org/about/terms.html>. JSTOR's Terms and Conditions of Use provides, in part, that unless you have obtained prior permission, you may not download an entire issue of a journal or multiple copies of articles, and you may use content in the JSTOR archive only for your personal, non-commercial use.

Please contact the publisher regarding any further use of this work. Publisher contact information may be obtained at <http://www.jstor.org/journals/rsl.html>.

Each copy of any part of a JSTOR transmission must contain the same copyright notice that appears on the screen or printed page of such transmission.

---

JSTOR is an independent not-for-profit organization dedicated to and preserving a digital archive of scholarly journals. For more information regarding JSTOR, please contact [support@jstor.org](mailto:support@jstor.org).

# The distribution of stress and velocity in glaciers and ice-sheets

By J. F. Nye

*H. H. Wills Physical Laboratory, University of Bristol*

*(Communicated by M. F. Perutz, F.R.S.—Received 20 August 1956  
—Read 8 November 1956)*

A block of ice resting upon a rough slope forms a theoretical model of a glacier or an ice-sheet, the sides of the glacier valley being ignored. Previous papers have described two types of steady flow in this model: (a) laminar flow, in which the longitudinal velocity gradient  $r$  is zero, and (b) extending or compressive flow, in which  $r$  is non-zero. (a) was derived under the assumption of a general flow law for ice, but (b) was only derived under the assumption of perfect plasticity. In the present paper a general flow law is used throughout, and the equations for steady flow, with  $r$  allowed to be non-zero, are found. The previous results (a) and (b) appear as special cases. Possible variations of density, temperature or flow law with depth are allowed for. If the density and the flow law are known as functions of depth in any region, and if the surface slope, the surface velocity, and the value of  $r$  are known, the equations give the stresses and velocity as functions of depth.

The borehole experiment on the Jungfraufirn (1948–50) allows an experimental test. From the observed value of  $r$ , and Glen's laboratory flow law for ice, a theoretical curve for the result of the experiment is calculated which is compared with the experimental curve. At a depth of 50 m the effect of ignoring  $r$ , as has been done hitherto, is to underestimate the shear rate by a factor of 50; on the present theory it is overestimated by a factor of 1.33. The remaining discrepancy is probably mainly due to the effect of the glacier sides.

## 1. INTRODUCTION

The motion of a glacier or an ice-sheet takes place partly by sliding on the rock bed and partly by a process of continuous distortion within the ice itself; the distortion is caused by the stresses set up in the ice by its own weight. In this paper we examine theoretically the distribution of stress and velocity within the moving mass and compare the result with experiment.

The flow law of ice has recently been investigated by Glen (1955), who applied uniaxial compressive stress to cylindrical polycrystalline specimens and measured the compressive strain rate. Prolonged application of a stress  $\sigma$  between 1 and 10 bars (1 bar =  $10^6$  dyn cm<sup>-2</sup>) produces a strain rate  $\dot{\epsilon}'$  given by

$$\dot{\epsilon}' = \left( \frac{\sigma}{A'} \right)^n, \quad (1)$$

where  $n$  equals 3.2 or 4.2 according to how the tests are interpreted, and  $A'$  is a constant for a given temperature. If ice behaved like a liquid showing Newtonian viscous behaviour,  $n$  would be equal to 1; if, on the other hand, it behaved like a perfectly plastic material—that is to say, if it had a sharp yield point and showed no subsequent strain-hardening, or strain-rate hardening— $n$  would be infinite and the yield stress would be  $A'$ . In fact, as the experiments show, ice is intermediate in behaviour between these two extremes.

We shall first consider, as a model of a glacier, a long parallel-sided slab resting on a uniformly inclined rough plane. It is simplest to assume that the flow in this model is laminar; that is, the upper layers shear over the lower layers so that each element is deformed in simple shear. This was the tentative assumption made by Gerrard, Perutz & Roch (1952) to interpret their measurement of the velocity distribution along a vertical line through a glacier. The equations for laminar flow under the flow law (1), which are quite straightforward, are given elsewhere (Nye 1952*a*).

In an earlier paper (Nye 1951), which will be referred to subsequently as (I), a different theoretical approach to the problem of flow in this model was made by idealizing the observed flow law to that of a perfectly plastic substance ( $n \rightarrow \infty$ ). It was found that laminar flow degenerates into 'plug flow'; the block moves down as a rigid body and all the shearing is concentrated into an infinitesimal layer at the bottom. But the main interest of the perfectly plastic case centres in the fact that, in addition to plug flow, two other sorts of flow are possible, called extending flow and compressive flow. In extending flow the forward velocity of the glacier increases as one goes down glacier, because the ice is being extended longitudinally; in compressive flow the velocity decreases because the ice is being compressed. In plug flow (and laminar flow) no longitudinal extension or compression occurs. In both extending and compressive flow the longitudinal velocity profile is one quadrant of an ellipse.

These solutions obtained for the perfectly plastic material seem to be of practical significance in glacier flow. In the first place, the extending solution leads to a natural explanation for the existence of transverse crevasses. Secondly, longitudinal extension and compression is commonly observed to take place in glaciers flowing in parallel-sided valleys—it would be surprising if it did not—and a theory of glacier flow should therefore include the effect. Moreover, the observed rates of strain associated with the extension or compression may be of the same order of magnitude as, or greater than, those due to the shearing motion of the upper layers over the lower; for example, the results from the Jungfraufirn described in § 10 show that the longitudinal rate of strain is greater than the tensor shear strain rate throughout almost the entire thickness of the glacier (down to a depth of 133 m in a total depth of 137 m).

It is therefore necessary to examine the connexion between the laminar flow obtained with the observed flow law and these other two types of flow obtained under the simplifying assumption of perfect plasticity. In particular, we may ask whether a type of flow may exist in glaciers in which some sort of extending or compressive flow is superimposed on a laminar flow. In the present paper we find that there are solutions of the flow equations which describe precisely this behaviour. Laminar flow turns out to be the special case in which the rate of longitudinal extension goes to zero. The theory is set up for a general relation between stress and strain rate, which can be specialized to the form (1) when required, and it proves possible to take account both of a variation of temperature and of density with depth. The previous results for perfect plasticity are included by allowing  $n$  to approach infinity, and in this way the transition from the perfectly plastic case to the more realistic

case with  $n$  equal to about 3 or 4 can be followed continuously. A feature of practical significance in the solutions is that they furnish an equation for the longitudinal velocity profile which can be checked in the field by a borehole experiment of the Gerrard, Perutz & Roch type.

## 2. GENERAL THEORY

The following general flow theory is the same as that already used for the analysis of the slow closing of glacier tunnels (Nye 1953) except that body-force terms are included from the beginning, and the restriction to homogeneous material is removed in order that the theory may be applicable to more general situations. There is a close formal similarity to the theory of plasticity (Hill 1950).

At a general point in the body let  $\rho$  be the density,  $\sigma_{ij}$  the components of stress, tensile stresses being positive, and  $u_i$  the components of velocity, with respect to rectangular Cartesian axes  $Ox_i$  fixed in space ( $i = 1, 2, 3$ ). The equations of slow, quasi-static motion of an element are then

$$\frac{\partial \sigma_{ij}}{\partial x_j} + \rho g_i = 0 \quad (i, j = 1, 2, 3), \quad (2)$$

the summation convention being used for repeated suffixes.  $g_i$  are the components of the gravitational acceleration  $g$ .

The rate of strain, or velocity gradient, tensor at the point has components

$$\dot{\epsilon}_{ij} = \frac{1}{2} \left( \frac{\partial u_i}{\partial x_j} + \frac{\partial u_j}{\partial x_i} \right). \quad (3)$$

We postulate, following the usual procedure of the theory of plasticity (Hill, chap. II), that the rate of strain tensor at a point is, to a first approximation, unaffected by a hydrostatic pressure superposed on the stress at the point. We therefore let  $\dot{\epsilon}_{ij}$  depend only on the deviatoric part of the stress tensor (the stress deviator) rather than on the stress tensor itself. The stress deviator has components

$$\sigma'_{ij} = \sigma_{ij} - \frac{1}{3} \delta_{ij} \sigma_{kk}, \quad (4)$$

where  $\delta_{ij} = 1$  if  $i = j$ , and  $\delta_{ij} = 0$  if  $i \neq j$ .

Next, assuming the material to be isotropic at every point, we postulate that the ratios of the strain-rate components depend only on the ratios of the components of the stress deviator and not on their absolute magnitudes. Thus we set

$$\dot{\epsilon}_{ij} = \lambda \sigma'_{ij}, \quad (5)$$

where  $\lambda$  is a scalar factor that depends in general on position and time. We note that this assumption implies incompressibility:  $\dot{\epsilon}_{ii} = 0$ . Equation (5) is analogous to the Lévy–Mises relations in the theory of plasticity. It is not the most general assumption that might be made for an isotropic material (see, for example, Truesdell 1950, 1952), but it is sufficiently general for the present purpose. Greater mathematical refinement is hardly justified at present in view of the other differences that exist between ice and our hypothetical material.

In order to introduce a flow law for the material we define an 'effective shear stress'  $\tau$ , and an 'effective strain rate'  $\dot{\epsilon}$  of an element, in terms of the second invariants of the stress deviator and the rate of strain tensor, thus

$$2\tau^2 = \sigma'_{ij}\sigma'_{ij}, \quad (6)$$

$$2\dot{\epsilon}^2 = \dot{\epsilon}_{ij}\dot{\epsilon}_{ij}, \quad (7)$$

both  $\tau$  and  $\dot{\epsilon}$  being always positive. This definition of  $\tau$  in terms of the second invariant corresponds to the Mises criterion of yielding in the theory of plasticity. (A more general flow theory would include the third invariant as well. The first invariant vanishes.)  $\tau$ , thus defined, equals  $\sqrt{\frac{3}{2}}$  times the octahedral shear stress.

We now postulate that for each element of ice a functional relationship exists between  $\dot{\epsilon}$  and  $\tau$ , namely,

$$\dot{\epsilon} = f(\tau). \quad (8)$$

This is the flow law. In some of the work we shall consider ice masses which are homogeneous in properties, so that the same function  $f(\tau)$  will apply at all points and all times. However, in more general cases, where the temperature, the texture and the density of the ice vary in space and time,  $f(\tau)$  will also vary. To take account of this we shall regard the spatial and temporal variation of the flow properties, caused by differences of temperature, texture and density, as given at the beginning of the problem. In other words we assume that sufficient physical conditions are known at each point to determine the flow law at the point. If, in addition, we have succeeded in finding  $\tau$ , then the flow law gives  $\dot{\epsilon}$ . (A more ambitious analysis would solve the heat-flow and the ice-flow problems together, but we shall not attempt this here.) This completes the postulates of our general theory.

(By using the stress deviator we have excluded any direct effect of hydrostatic pressure on the flow. But it may be noted in passing that, if the distribution of hydrostatic pressure is known in advance, any effect it might have on the flow properties could be included in exactly the same way as the effect of any other non-uniformity, that is, by allowing  $f(\tau)$  to change from point to point.)

At any point we have, from (7), (5) and (6),

$$2\dot{\epsilon}^2 = \lambda^2 \sigma'_{ij}\sigma'_{ij} = 2\lambda^2 \tau^2,$$

and therefore

$$\dot{\epsilon} = \lambda \tau. \quad (9)$$

The value of  $\lambda$  is thus  $f(\tau)/\tau$ , and so from (3) and (5) we obtain

$$\frac{1}{2} \left( \frac{\partial u_i}{\partial x_j} + \frac{\partial u_j}{\partial x_i} \right) = \frac{f(\tau)}{\tau} \sigma'_{ij}. \quad (10)$$

Equations (10), where  $\tau$  and  $\sigma'_{ij}$  are given by (6) and (4), together with equations (2), form nine equations for the determination of the values of the nine unknowns  $\sigma_{ij}$  and  $u_i$  at any instant.

*Special case of power law.* If, as suggested by Glen's experiments already referred to,

$$f(\tau) = \left( \frac{\tau}{A} \right)^n, \quad (11)$$

where, for a given element of ice at a given temperature,  $A$  and  $n$  are constants, we have

$$\lambda = \frac{\tau^{n-1}}{A^n}. \quad (12)$$

For  $n = 1$  the equations reduce to those for an incompressible Newtonian liquid of viscosity  $\frac{1}{2}A$ ; while for  $n \rightarrow \infty$ , as discussed elsewhere (Nye 1953), the equations reduce to those for a perfectly plastic material of constant yield stress  $\tau = A$ . Ice thus appears as intermediate in flow properties between these two extremes. For the special case of uniaxial compression this last conclusion follows directly from Glen's experiments, as we have seen. The theory outlined above represents, in effect, the simplest, but not the only possible generalization of the same result to three-dimensional states of flow.

### 3. EQUATIONS FOR PLANE STRAIN

We write  $x, y, z$  for  $x_i$ ;  $u, v, w$  for  $u_i$ ;  $\sigma_x, \sigma_y, \sigma_z, \tau_{xy}, \tau_{yz}, \tau_{zx}$  for  $\sigma_{ij}$ ;  $\dot{\epsilon}_x, \dot{\epsilon}_y, \dot{\epsilon}_z, \dot{\epsilon}_{xy}, \dot{\epsilon}_{yz}, \dot{\epsilon}_{zx}$  for  $\dot{\epsilon}_{ij}$ . Take  $Oz$  horizontal, so that  $g_3 = g_z = 0$ , and consider a state of plane strain in which movement is confined to the  $xy$  plane. The velocities and stresses at any instant are functions of  $x$  and  $y$  only, and we have  $w = 0, \tau_{zx} = \tau_{yz} = 0$ . Hence the first two of equations (2) become

$$\frac{\partial \sigma_x}{\partial x} + \frac{\partial \tau_{xy}}{\partial y} + \rho g_x = 0, \quad (13)$$

$$\frac{\partial \tau_{xy}}{\partial x} + \frac{\partial \sigma_y}{\partial y} + \rho g_y = 0. \quad (14)$$

Since  $\dot{\epsilon}_z = 0$ , it follows from (5) that  $\sigma'_z = 0$ , and hence, from (4),  $\sigma_z = \frac{1}{2}(\sigma_x + \sigma_y)$ . The remainder of equations (5) become

$$\frac{\partial u}{\partial x} = -\frac{\partial v}{\partial y} = \frac{1}{2}\lambda(\sigma_x - \sigma_y), \quad \frac{1}{2}\left(\frac{\partial v}{\partial x} + \frac{\partial u}{\partial y}\right) = \lambda\tau_{xy}, \quad \frac{\partial u}{\partial z} = \frac{\partial v}{\partial z} = 0. \quad (15)$$

Finally, equations (6) and (7) take the form

$$4\tau^2 = (\sigma_x - \sigma_y)^2 + 4\tau_{xy}^2, \quad (16)$$

and

$$2\dot{\epsilon}^2 = \left(\frac{\partial u}{\partial x}\right)^2 + \left(\frac{\partial v}{\partial y}\right)^2 + \frac{1}{2}\left(\frac{\partial v}{\partial x} + \frac{\partial u}{\partial y}\right)^2. \quad (17)$$

We may note in passing that, since each element is deformed in pure shear, only the relation between the stress on an element and the strain rate in pure shear is needed—not the full relationship applicable to a general stress situation.

### 4. THE FIRST MODEL AND THE STRESS SOLUTION

The first model to be considered (figure 1) is a block of ice of infinite extent and uniform thickness resting on an inclined rough plane of slope angle  $\alpha$ . The problem is to calculate the possible distributions of stress and velocity, at any instant, for the slow flow of the block.

Take axes with the origin on the upper surface of the block, with  $Oz$  horizontal (as before), with  $Ox$  pointing down the line of greatest slope and with  $Oy$  perpendicular to the surface and pointing downwards. Then

$$g_x = g \sin \alpha, \quad g_y = g \cos \alpha. \quad (18)$$

Movement is supposed to be entirely in the  $xy$  plane. We take  $\rho$  to be a known function of  $y$  but to be independent of  $x$ .

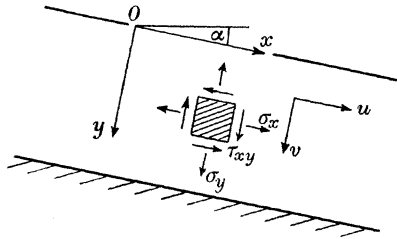


FIGURE 1. The first model, showing notation and the positive sense of the stress components.

The assumption is now made that both  $\tau$  and  $\tau_{xy}$  are functions of  $y$  only and not of  $x$ . This step is crucial, for it makes possible a self-consistent solution of the equations in two stages. First, we find a stress solution of equations (13) and (14) in terms of  $\tau$ , which is thus far an undetermined function of position. Secondly, we substitute this stress solution into equations (15) and so obtain a velocity solution, which will also be in terms of  $\tau$ . The velocity solution is then used to find the distribution of  $\dot{\epsilon}$ , again in terms of  $\tau$ . Then by using the functional relationship (8) we obtain the distribution of  $\tau$ . The stress and velocity solution is then determinate.

The stress solution referred to is closely similar to that given by Prandtl (1923) and discussed by Nádai (1931) for a block of perfectly plastic weightless material compressed between two parallel rough plates. In the Prandtl solution  $\tau$  is a constant and there are no gravity terms. However, it is found that a variation of  $\tau$  with  $y$  may be introduced without essentially changing the form of the solution. The effect of the gravity terms has already been dealt with in (I) for constant  $\rho$ ; but in a similar way it turns out that a variation of  $\rho$  with  $y$  does not cause any essential difficulty. The stress solution is as follows:

$$\left. \begin{aligned} \sigma_x &= -\bar{\rho}g_y y \pm 2\sqrt{\{\tau^2 - (\bar{\rho}g_x y)^2\}}, \\ \sigma_y &= -\bar{\rho}g_y y, \\ \tau_{xy} &= -\bar{\rho}g_x y, \end{aligned} \right\} \quad (19)$$

where  $\bar{\rho}$  is the average density between the depth  $y$  and the surface  $y = 0$ , so that  $\bar{\rho}y = \int_0^y \rho dy$ . The boundary conditions used are that on  $y = 0$ ,  $\tau_{xy} = 0$  and  $\sigma_y = 0$  (the effect of atmospheric pressure would be simply to add a constant to  $\sigma_x$  and  $\sigma_y$ ).

If the material is perfectly plastic,  $n \rightarrow \infty$  and  $\tau$  is a constant, and if  $\rho$  is also a constant ( $\equiv \bar{\rho}$ ) the solution reduces to that given in (I). The choice of signs before the square root in fact gives two solutions. The upper sign corresponds to the active

Rankine state in soil mechanics and to 'extending flow', while the lower sign corresponds to the passive Rankine state and to 'compressive flow'. Henceforth the terms extending and compressive flow will be used for the two solutions even when  $\tau$  is not a constant; and whenever there is a choice of signs in the expressions that follow, the upper sign will refer to extending and the lower sign to compressive flow. All radicals are to be taken positive.

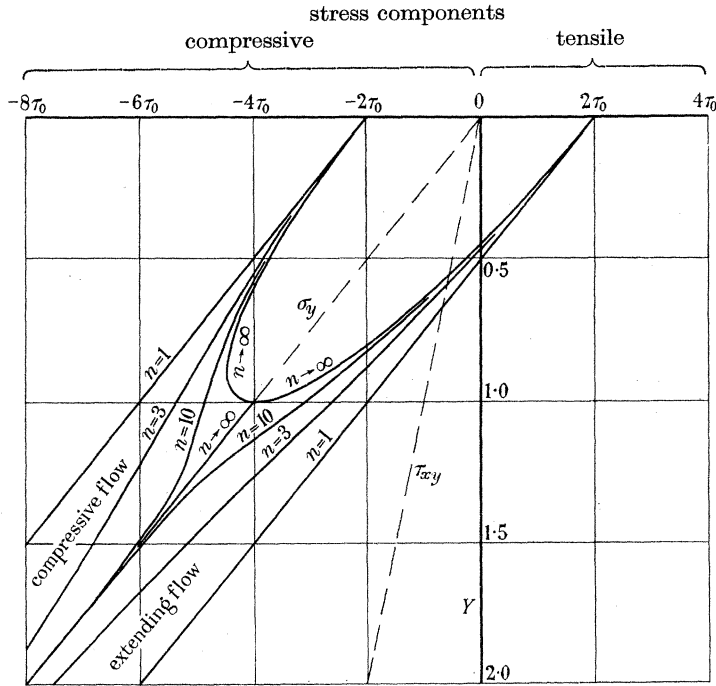


FIGURE 2. Stress components as functions of depth  $Y$ , measured in dimensionless units, for uniform density and a power law of flow. The distribution of  $\sigma_x$  is given by the double family of full curves; each value of  $n$  gives one curve for extending flow and one for compressive flow. The distributions of  $\sigma_y$  and  $\tau_{xy}$  are shown by the broken lines and are the same for all  $n$ . All curves are drawn for a slope of  $\alpha = 14^\circ 2'$  ( $\cot \alpha = 4$ ) and the units are such that  $c = 1$ .

The variation of  $\sigma_x$ ,  $\sigma_y$  and  $\tau_{xy}$  with depth is shown in figure 2 for  $\rho$  constant. The depth is measured in dimensionless units to be defined later. The curves for  $\sigma_x$  cannot be established until  $\tau$  is known as a function of  $y$ , except for the semi-ellipse corresponding to  $n \rightarrow \infty$ . This curve, already known from (I), may be deduced immediately by putting  $\tau$  constant in (19).

### 5. THE VELOCITY SOLUTION

Solutions of equations (15), using the expressions for the stress components given by (19), can be found by taking  $\partial v / \partial x = 0$ , an assumption which is compatible with the condition  $v = 0$  at the lower surface of the block. Then we have

$$\frac{\partial u}{\partial x} = -\frac{\partial v}{\partial y} = \pm \lambda \sqrt{\{\tau^2 - (\bar{\rho} g_x y)^2\}}, \quad \frac{\partial u}{\partial y} = -2\lambda \bar{\rho} g_x y. \tag{20}$$



Equations (20) may be integrated as follows. Eliminate  $\lambda$  to give

$$\frac{\partial u}{\partial y} = \pm \frac{2\bar{\rho}g_x y}{\sqrt{\{\tau^2 - (\bar{\rho}g_x y)^2\}}} \frac{\partial v}{\partial y}. \quad (21)$$

Then, differentiating with respect to  $x$  and putting  $\partial v/\partial x = 0$ , we have  $\partial^2 u/\partial x \partial y = 0$ , and hence  $\partial^2 v/\partial y^2 = 0$ . We thus write

$$v = a_1 y + a_2,$$

where  $a_1$  and  $a_2$  are constants for the instant considered.

We now have, using (21),

$$\frac{\partial u}{\partial x} = -\frac{\partial v}{\partial y} = -a_1, \quad \frac{\partial u}{\partial y} = \pm \frac{2a_1 \bar{\rho}g_x y}{\sqrt{\{\tau^2 - (\bar{\rho}g_x y)^2\}}},$$

and, integrating,

$$u = -a_1 x \pm 2a_1 g_x \int_0^y \frac{\bar{\rho} y \, dy}{\sqrt{\{\tau^2 - (\bar{\rho}g_x y)^2\}}} + (u)_0,$$

where  $(u)_0$  is the value of  $u$  at the origin.

From equations (20),  $\lambda$  is given by

$$\lambda = \mp \frac{a_1}{\sqrt{\{\tau^2 - (\bar{\rho}g_x y)^2\}}}.$$

Now, for a positive rate of work at every point,  $\lambda$  must be positive. We therefore give  $a_1$  the values  $\mp r$ , where  $r$  is a positive constant.  $r$  is equal to the longitudinal strain rate of the block, for  $\partial u/\partial x = \pm r$ . The velocity solution at any instant is thus

$$\left. \begin{aligned} u &= \pm rx - 2rg_x \int_0^y \frac{\bar{\rho} y \, dy}{\sqrt{\{\tau^2 - (\bar{\rho}g_x y)^2\}}} + (u)_0, \\ v &= \mp r(y-h), \end{aligned} \right\} \quad (22)$$

where  $h$  is the thickness of the block;  $a_2$  has been chosen so that  $v = 0$  on the lower surface (loss of ice by melting at the lower surface could readily be allowed for by adjusting  $a_2$ ). We note that the velocity components at the upper surface ( $y = 0$ ) are

$$u = \pm rx + (u)_0, \quad v = \pm rh.$$

It is interesting that the linear variation of  $v$  with depth, already familiar from the perfectly plastic case, is preserved in spite of the variable  $\rho$  and  $\tau$ .

To evaluate the integral in the expression for  $u$  we need to know  $\bar{\rho}$  and  $\tau$  as functions of  $y$ .  $\bar{\rho}$  is supposed given as one of the conditions of the problem;  $\tau$  at each point is determined by the flow law of the ice at that point and by the effective strain rate  $\dot{\epsilon}$ .  $\dot{\epsilon}$  is found from (17) as

$$\dot{\epsilon}^2 = r^2 + \frac{1}{4} \left( \frac{\partial u}{\partial y} \right)^2, \quad (23)$$

and so, using the value of  $\partial u/\partial y$  now obtained,

$$\dot{\epsilon} = \frac{r\tau}{\sqrt{\{\tau^2 - (\bar{\rho}g_x y)^2\}}} = f(\tau). \quad (24)$$

Thus  $\dot{\epsilon}$  does not depend on  $x$  and, to be consistent, we must stipulate that the form of the function  $f(\tau)$ , hitherto allowed to vary from point to point of the material, does not depend on  $x$ . If the constant  $r$  is given, if  $\bar{\rho}$  is known as a function of depth  $y$ , and if the form of  $f(\tau)$  is known for each depth, equation (24) allows  $\tau$  to be determined for each depth. The integral in (22) may then be evaluated and hence the velocity distribution determined.

A more compact expression for  $u$  is obtained by substituting from (24) into (22); thus

$$u = \pm rx - 2g_x \int_0^y \frac{f(\tau)}{\tau} \bar{\rho} y dy + (u)_0. \quad (25)$$

## 6. SPECIAL CASE: POWER LAW AND UNIFORM DENSITY

To make clearer the meaning of the solutions it is useful to consider the special case when  $f(\tau)$  has the form (11),  $A$  and  $n$  having the same values for all points of the block, and when  $\rho$  is constant; for the integration in (22) can then be performed analytically. In this case equation (24) may be written

$$\frac{f(\tau)}{\tau} = \frac{\tau^{n-1}}{A^n} = \frac{r}{\sqrt{\{\tau^2 - (\bar{\rho}g_x y)^2\}}}. \quad (26)$$

It is convenient to introduce units of strain rate, stress, length and velocity which are characteristic for the problem. First define a unit of strain rate  $r_0$  by

$$r = cr_0, \quad (27)$$

where  $c$  is dimensionless.  $r_0$  here has an arbitrary value; but for most purposes  $c$  will be taken as equal to 1, so that the unit of strain rate chosen is simply the longitudinal strain rate of the block  $r$ . However, we shall later want to consider the special case where  $r$  is zero, and so  $c$  is introduced to prevent our unit of strain rate becoming zero.

Let the unit of stress  $\tau_0$  be given by

$$r_0 = \left(\frac{\tau_0}{A}\right)^n.$$

Let the unit of length be  $l_0 = \tau_0/\rho g_x$  and the unit of velocity  $v_0 = r_0 l_0$ . Hence we define the dimensionless variables

$$T = \frac{\tau}{\tau_0}; \quad X = \frac{x}{l_0}, \quad Y = \frac{y}{l_0}; \quad U = \frac{u}{v_0}, \quad V = \frac{v}{v_0}.$$

The velocity solution (22) is then written

$$U = \pm cX - 2c \int_0^Y \frac{Y dY}{\sqrt{(T^2 - Y^2)}} + (U)_0, \quad (28)$$

$$V = \mp c(Y - Y_{\text{bed}}). \quad (29)$$

Equation (26) takes the form

$$T^{n-1} = \frac{c}{\sqrt{(T^2 - Y^2)}}, \quad (30)$$

an equation which gives the effective stress  $T$  as a function of depth  $Y$ . Taking  $c = 1$ , this relation is plotted in figure 3 for  $n = 1, 3, 10$  and  $n \rightarrow \infty$ ;  $T = Y$  is an asymptote of all the curves. The curve for  $n = 1$  is part of a rectangular hyperbola.

The integral in (28) is now evaluated by using  $T$  as the variable. From (30)

$$Y^2 = \frac{T^{2n} - c^2}{T^{2(n-1)}}, \tag{31}$$

and so we obtain

$$U = \pm cX - 2 \int_{c^{1/n}}^T \{T^n + c^2(n-1)T^{-n}\} dT + (U)_0,$$

and, carrying out the integration,

$$U = \pm cX - \frac{2}{n+1} \{T^{n+1} - c^2(n+1)T^{1-n} + nc^{1+1/n}\} + (U)_0. \tag{32}$$

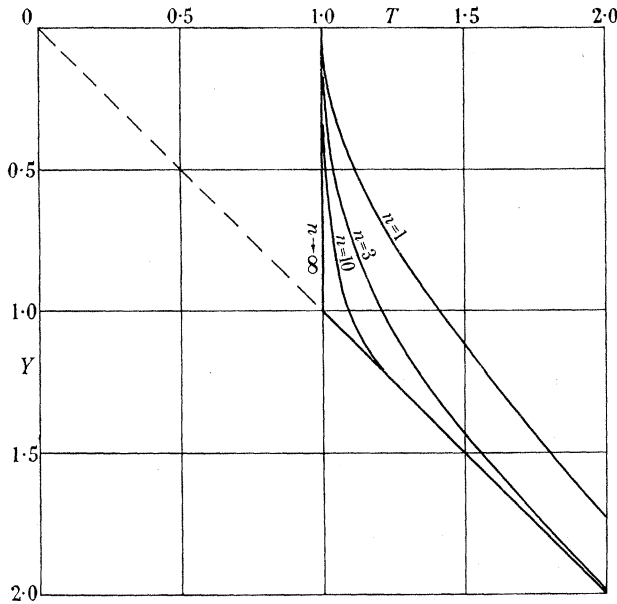


FIGURE 3. Effective shear stress  $T$  as a function of the depth  $Y$ , both quantities being expressed non-dimensionally, for uniform density and a power law of flow.  $c$  is taken equal to 1.

$T$  can be eliminated between (31) and (32) so as to give  $U$  as a function of  $X$  and  $Y$ , but the resulting expression is long and clumsy. It is better to regard  $T$  as an independent parameter connecting  $U$  with  $X$  and  $Y$  through the two equations. Taking  $c = 1$ , curves of  $U$  as a function of  $Y$  are plotted in figure 4 for various values of  $n$ . If  $r, A, n, \rho$  and  $g_x$  are specified, the curves in figure 4 give the longitudinal velocity profile of the block, except for an additive constant directly proportional to  $x$ .

*Limiting cases*

(i) *Longitudinal strain-rate zero*

We treat the case  $r = 0$  by putting  $c = 0$ . In equation (30), since  $T$  cannot be zero everywhere, we must have  $T = Y$  for all  $Y$  and  $n$ . Hence the velocity distribution (32) and (29) takes the simple form

$$U = -\frac{2}{n+1} Y^{n+1} + (U)_0, \quad V = 0.$$

In terms of measurable quantities this is

$$u = -\frac{2}{n+1} \left( \frac{\rho g_x}{A} \right)^n y^{n+1} + (u)_0, \quad v = 0, \quad (33)$$

which is the velocity distribution for laminar flow (Nye 1952*a*, equation (2)).

The only reason for introducing  $c$  in equation (27) was to make possible this demonstration that laminar flow is a particular case of the more general velocity

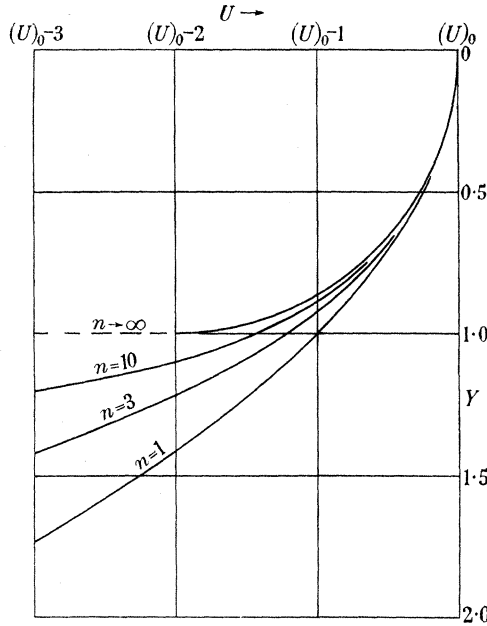


FIGURE 4. Longitudinal velocity  $U$  as a function of depth  $Y$ , both quantities being expressed non-dimensionally, for uniform density and a power law of flow. The curves are drawn for  $X = 0$ ;  $(U)_0$  is the surface velocity at  $X = 0$ .  $c$  is taken equal to 1.

distribution for extending and compressive flow. For all other cases we may take  $c$  equal to 1 without loss of generality, and henceforth we shall do so, putting therefore  $r_0 = r$ .

(ii) *Newtonian liquid* ( $n = 1$ , viscosity  $\frac{1}{2}A$ )

Here equation (31) becomes  $Y^2 = T^2 - 1$ ,

and (32) gives  $U = \pm X - Y^2 + (U)_0$ .

Thus, in terms of the original variables, the velocity distribution is

$$u = \pm rx - \frac{\rho g_x}{A} y^2 + (u)_0, \quad v = \mp r(y-h). \quad (34)$$

This parabolic relation between  $u$  and  $y$  is the same as is obtained by putting  $n = 1$  in equation (33) for laminar flow. Thus, when  $n = 1$  the presence of the longitudinal strain rate  $r$  does not essentially alter the velocity profile; the motion is simply

laminar flow with a uniform longitudinal and vertical strain rate superimposed upon it. It is hardly surprising that such a linear superposition of motions does not take place when the flow law is not linear.

(iii) *Perfect plasticity* ( $n \rightarrow \infty$ , yield stress =  $A = \tau$ )

As  $n \rightarrow \infty$ ,  $T \rightarrow 1$  for  $Y \leq 1$  and  $T \rightarrow Y$  for  $Y > 1$  (figure 3). The limit must be approached cautiously. For the region  $Y \leq 1$  we cannot simply put  $T = 1$  and  $n$  infinite in (31) and (32) because  $T^n$  approaches different values for different  $Y$ . Instead we return to (28) and (29), put  $T = 1$  and integrate to obtain

$$U = \pm X + 2\{\sqrt{(1 - Y^2)} - 1\} + (U)_0 \quad \text{if } 0 \leq Y \leq 1; \quad U \rightarrow \infty \quad \text{if } Y > 1;$$

$$V = \mp (Y - Y_{\text{bed}}).$$

The velocity profile for  $0 \leq Y \leq 1$  is thus one quadrant of an ellipse, as shown in figure 4, and as already found in the previous analysis (equation (9) of (I)).

## 7. THE STRESS DISTRIBUTION

### (i) *General flow law*

Since  $\tau$  is now known as a function of  $y$  the first of equations (19) gives  $\sigma_x$  as a function of  $y$ .

### (ii) *Power law and uniform density*

We write the first of equations (19) in the system of dimensionless variables (with  $\rho$  constant) as

$$\sigma_x/\tau_0 = -Y \cot \alpha \pm 2\sqrt{(T^2 - Y^2)}.$$

$T$  being known as a function of  $Y$  (figure 3), this equation gives  $\sigma_x/\tau_0$  as a function of  $Y$ ; the relation is plotted in figure 2 for an arbitrary slope of  $14^\circ 2'$  ( $\cot \alpha = 4$ ). On  $Y = 0$ ,  $\sigma_x = \pm 2\tau_0$  for all values of  $n$ . The characteristic unit of stress  $\tau_0$  may thus be identified as one-half of the longitudinal stress in the surface.

When  $n = 1$ ,  $\sigma_x$  is readily seen to be linear in  $y$ , as might be expected in view of the straightforward superposition of motions that occurs in this case. When  $n \rightarrow \infty$  the curve for  $\sigma_x$  ( $0 \leq Y \leq 1$ ) is part of an ellipse, as already noted.

## 8. DISCUSSION

The solutions obtained for the cases where  $n$  lies between 1 and infinity are very similar in their general features to those already found in (I) for the perfectly plastic material. It thus appears that, unless  $r = 0$ , and apart from any addition or subtraction of material at the upper surface, the block is either uniformly thinning or thickening according to whether the upper or the lower sign is taken in the various expressions. Since there is no change in volume, this must necessarily be accompanied by a longitudinal extension or contraction of the block as a whole, represented by the term  $\pm rx$  in the first of equations (22). Just as for a perfectly plastic material, the distribution of  $u$  with depth is independent of the sign of the longitudinal strain rate.

No boundary conditions on the tangential velocity, or on the shear stress, have so far been imposed at the lower surface of the block. This question will be taken up

below. It would appear that, provided the constant in the expression for  $v$  is suitably adjusted, the solution can be extended downwards from the upper surface indefinitely, and that we are free to place the lower boundary at whatever depth we like.

The main feature of a real glacier that is omitted in our model is the variation in the  $z$  direction—that is to say, the influence of the valley walls. The greater the width of the glacier in comparison with its depth the better the approximation, and for an ice-sheet the approximation should be very good. A discussion of the general effect of the valley walls has been given in other papers (Nye 1952*a, b*).

The quantity  $r$  is fairly easily measured directly on a glacier. Once it is known the longitudinal velocity profile can be calculated. In real glaciers and ice-sheets—the word glacier will refer to both in most of what follows—the slope and other conditions of course vary with  $x$ , and are not constant as in our model. However, our solution should approximate to the true state of affairs even when the slope and other conditions do change, provided the changes are small in a distance equal to the thickness of the glacier. This has been shown in detail for the perfectly plastic case, and presumably it is also true for the more general case. From this point of view the present theory is to be regarded as giving essentially the local differential motions of a glacier. Thus the variation of  $u$  with  $y$  calculated with the local values of the various parameters should be a good approximation. The linear variation of  $u$  with  $x$ , on the other hand, cannot be expected to hold in a real glacier for any considerable distance.

When deciding what values of the various parameters should be used at a particular place on a real glacier, the question arises as to what value of the slope to use; for, in general, the slope of the upper surface  $\alpha_1$ , say, and of the bed  $\alpha_2$ , say, will be different. It is assumed that  $(\alpha_1 - \alpha_2)$  is small. The question of which to use is not important if both  $\alpha_1$  and  $\alpha_2$  individually are large compared to their difference, but the distinction becomes critical if  $\alpha_1$  and  $\alpha_2$  individually are of the same order as the difference between them. As an extreme example of this consider an ice-sheet resting on a horizontal bed, so that  $\alpha_2 = 0$ . The difference between putting  $\tau_{xy} = -\bar{\rho}gy \sin \alpha_1$  and  $\tau_{xy} = -\bar{\rho}gy \sin \alpha_2$  is then the difference between having a finite driving force for the shear motion and none at all. In fact it is the slope of the upper surface that must be used, as can be seen as follows. If, in the model with which we started,  $\alpha_1$  is the slope of the upper surface, the whole analysis proceeds with this value, the  $x$  axis is parallel to the upper surface, and the solution is developed from the upper surface downwards. Finally, we have to terminate the solution by inserting the bed of the glacier. If the slope of this is  $\alpha_1$  there is no difficulty. If, however, the slope of the bed  $\alpha_2$  is slightly different from  $\alpha_1$  the stress and velocity solutions are still good approximations, provided a small modification is made in the velocity solution. The modification is necessary because the boundary condition on the bed is no longer  $v = 0$ , but that the velocity should be parallel to the bed. The matter is put right by adding to  $v$  a component equal to  $u(\alpha_2 - \alpha_1)$ . (Note that, if  $r = 0$ , this addition makes the velocity parallel to the bed at all depths.)

The result of the analysis as it applies to real glaciers may therefore be expressed

as follows. We neglect the influence of the valley sides and postulate that no rapid changes take place in the longitudinal direction. The approximate stress distribution is then as given in (19) with  $\tau$  given by (24). The approximate velocity distribution is

$$\left. \begin{aligned} u &= u_{\text{surface}} - 2g_x \int_0^y \frac{f(\tau)}{\tau} \bar{\rho} y dy, \\ v &= \mp r(y-h) + u(\alpha_2 - \alpha_1). \end{aligned} \right\} \quad (35)$$

It is natural to ask what in fact determines  $r$ , the longitudinal strain rate, regarded up to now as a parameter to be found empirically. In the perfectly plastic model the problem can be solved explicitly (see (I)) because the solution naturally terminates when  $\tau_{xy}$  reaches the value of the critical shear stress. If we postulate that the depth of the glacier is equal to this critical depth everywhere we have immediately†  $h = h_0/\sin \alpha_1$ , where  $h_0 = A/\rho g$ , at all points down the glacier. The thickness of the glacier must therefore adjust itself to the slope. If there is no addition or subtraction of material at the upper surface, the thickness change is accomplished by a longitudinal strain rate which is readily shown to be  $(\phi/hR) \cot \alpha_1$ , where  $\phi$  is the total flow rate (volume, per unit thickness in the  $z$  direction, flowing in unit time through a cross-section perpendicular to  $Ox$ ), and  $R$  is the radius of curvature of the surface.  $R$  is positive when the surface is convex and negative when concave. If, on the other hand, the slope is uniform but ice is being added or subtracted at the upper surface by snowfall or ablation at the rate  $d\phi/dx$  (measured as the thickness of ice per unit time), a longitudinal strain rate of  $h^{-1}d\phi/dx$  is necessary to maintain the critical thickness. In general

$$r = \pm \frac{1}{h} \left( \frac{d\phi}{dx} + \frac{\phi}{R} \cot \alpha_1 \right). \quad (36)$$

It must be emphasized that equation (36) is founded on the condition that  $\tau_{xy}$  is constant on the bed of the glacier. When  $n$  is not infinite there is nothing in the analysis which demands such a condition. Nevertheless, as mentioned below,  $\tau_{xy}$  does appear to be approximately constant on the bed of a glacier. It is therefore plausible that equation (36) gives some approximation to the value of  $r$  in real glaciers.

It is possible to understand how  $r$  is determined in nature by looking at the forces involved rather than at the velocities, and using an argument due to Orowan (1949). In our solution the downhill component of the weight of the glacier,  $\bar{\rho}gh \sin \alpha_1$ , is balanced essentially by the uphill tangential force exerted by the bed on the ice.

But there must be places where the balance is slightly disturbed; and  $\int (\tau_{xy})_{\text{bed}} dx$ , taken from the head of the glacier to a given  $x$ , will not then exactly balance

† In (I) this formula was derived explicitly only for a glacier, the formula for an ice-sheet being somewhat different. However, the difference is removed if in (I) the origin is shifted to the upper surface of the block and the  $x$  axis is taken parallel to the upper surface. The stress and velocity solutions are then essentially unaltered, except that  $\alpha$  and  $R$  refer to the upper surface rather than to the bed. On the other hand, in equation (10) of (I) the first term in  $dh/dx$  does not appear, and so the condition  $h = h_0/\sin \alpha$  applies not only to the glacier but also to the ice-sheet. The two cases are thus really one and the same.

$\int \bar{\rho}gh \sin \alpha_1 dx$ . The difference between the integrals will result in an excess longitudinal component of stress  $\sigma_x$ , in addition to the hydrostatic component  $\bar{\rho}g_y y$  which is always present. It is this excess component that causes the longitudinal strain rate.

*Boundary conditions on the lower surface*

As mentioned above, the present approach does not give any criterion for fixing the thickness of the glacier, except when  $n \rightarrow \infty$ . The problem in its simplest form is illustrated in figure 5. In a steady state the total flow rate is determined by the rate of accumulation and ablation integrated over all parts of the glacier above the place we are considering. At this place let us assume, for simplicity, that the flow is laminar and that there is no accumulation or ablation. Then the slope of the valley determines the shape of the  $u:y$  curve. The thickness, however, as the figure shows, is still undetermined; for a given  $\phi$  could be achieved either by a thin glacier slipping fast on its bed, or by a thicker glacier in which there is more differential motion within the ice.

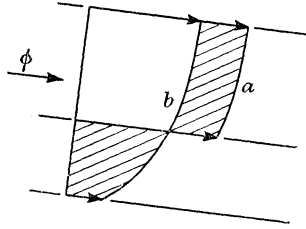


FIGURE 5. A given discharge  $\phi$  can be achieved (a) by a thin glacier slipping fast on its bed, or (b) by a thicker glacier of equal slope in which there is more differential motion within the ice. Shaded areas are equal.

There is no reason to suppose that the condition  $u = 0$  at the lower surface, which would be usual for a Newtonian liquid, should hold for ice sliding over rock; and, in fact, direct observation (McCall 1952) shows that sliding does occur and may sometimes be the major part of the total motion. It is more reasonable to think that, with given thermal conditions and a bed of given roughness or relief, there is a functional relationship between  $\tau_{xy}$  and  $u$  on the bed. In that case a change of  $u$  with  $x$  on the bed, which is almost inevitable, would imply a change of  $\tau_{xy}$  with  $x$ —and this would vitiate the solutions we have found for extending and compressive flow. But the difficulty is perhaps not serious, for the truth may be that  $\tau_{xy}$  on the bed is indeed governed partly by the velocity of sliding, but, owing to the high value of  $n$ , a change in  $u$  on the bed only causes a relatively small change in the shear stress. In support of this view, when the values of  $\tau_{xy}$  on the beds of glaciers and ice-sheets are calculated from the measured thicknesses and surface slopes, they show remarkably little variation from point to point of the same glacier, and even from one glacier to another (Nye 1952*a, b, c*; Orvig 1953; Robin 1953; Bauer 1955; Ward 1955; Bull 1957).



## 9. TRANSVERSE CREVASSES

In extending flow figure 2 shows that there is an upper layer of the glacier where  $\sigma_x$  is tensile. Explicitly,  $\sigma_x$  is tensile to a depth  $y$ , where

$$\bar{\rho}gy = 2\tau(3\sin^2\alpha_1 + 1)^{-\frac{1}{2}}, \quad (37)$$

and  $\tau$  is given by (24). In most cases the value of  $\tau$  will be close to its value on the surface, that is,  $\tau$  will be given sufficiently accurately by  $f(\tau) = r$ . Crevasses will occur within the tensile layer when the tension exceeds the fracture strength. The effect of atmospheric pressure is to add a (negative) constant on to  $\sigma_x$  and  $\sigma_y$ , but it will not alter the depth of the crevasses (Nye 1955).

## 10. REINTERPRETATION OF THE JUNGFRAUFIRN BOREHOLE EXPERIMENT

In a well-known experiment Gerrard *et al.* (1952) have measured directly the variation of longitudinal velocity  $u$  with depth  $y$  in a glacier. Working on the Jungfrau firn, in the Bernese Oberland, they melted a vertical hole, 137 m long, from the glacier surface to the rock bed. The hole was lined with a 3 in. steel tube which became tilted and bent according to the variation of  $u$  with  $y$ . The inclination of the tube at different depths was measured at the beginning of the experiment in August 1948, and again in October 1949 and September 1950. The experiment thus gives directly the rate of change of inclination of the pipe as a function of depth, and the result was straightforwardly interpreted as giving the rate of shear strain  $\partial u/\partial y$ , which will be denoted by  $\dot{\gamma}$ , as a function of  $y$ .

The variation of density with depth was not measured at the boring site but had been measured down to a depth of 28 m in 1938 in the wall of a crevasse which happened to be at the same altitude as the boring site and on the same glacier. By use of these data a density curve for the whole depth of the glacier was inferred, and then, using the measured surface slope,  $\bar{\rho}g_x y$  was calculated as a function of  $y$ . The result of the experiment was thus a relation between  $\dot{\gamma}$  and  $\bar{\rho}g_x y$ . It was found that  $\dot{\gamma} \propto (\bar{\rho}g_x y)^n$ , where  $n \sim 1.5$ ; whereas if the glacier were deforming by laminar flow, as was tentatively assumed, Glen's experiments would lead one to expect a value of  $n$  of about 3 or 4.

It seemed possible that the discrepancy was due to the erroneous assumption of laminar flow (Nye 1953; Perutz 1954; Glen 1955) and this can now be checked. Ing. P. Kasser has measured the spatial variation of the surface velocity at the borehole site.† The movement of two stakes set in the surface along a line of flow was measured from 2 September 1949 to 5 September 1950. In this period (368 days) the distance between the stakes increased from 27.3 to 31.4 m. The tensile strain rate is then  $r = (1/t) \ln(l_2/l_1) = 0.14 \text{ yr}^{-1}$ . The positive sign was to be expected from the presence of a few transverse crevasses in the region of the boring site. Tilting of the stakes may cause an error in the measured extension, but Kasser reports that it will not exceed 0.5 m. Thus for the second year of the pipe observations we may take

$$r = 0.14 \pm 0.02 \text{ yr}^{-1} \quad (\text{maximum error}).$$

† I am much indebted to Ing. Kasser for making the results of his work available to me.

The corresponding values of  $r$  for later periods, measured at the same absolute position (and so necessarily on different stakes), are as follows:

dates	8. ix. 52	8. ix. 53	22 vi. 54	25 ix. 54	13. xii. 54	24. i. 55	31. iii. 55
period (days)	365	288	95	79	42	66	
$r$ yr <sup>-1</sup>	0.12	0.16	0.25 (?)	0.12 (?)	0.17	0.18	

(The maximum error in  $r$  due to tilting of the stakes is  $\pm 0.01$  in each case.)

With  $r$  known, and with  $\dot{\gamma}$  known as a function of  $\bar{\rho}g_x y$  from the pipe experiment, it is possible, in principle, to deduce a flow law from the experiment by using the equations

$$\dot{\epsilon} = \sqrt{(r^2 + \frac{1}{4}\dot{\gamma}^2)}, \quad \tau = -\bar{\rho}g_x y \frac{2\dot{\epsilon}}{\dot{\gamma}}, \tag{38}$$

which are readily derived from (23) and (24) (putting  $\partial u/\partial y = \dot{\gamma}$ ). However, in the upper parts of the pipe  $\dot{\gamma}$  is small compared with  $r$  and difficult to measure. Hence, a large proportional error in  $\dot{\gamma}$  in the upper parts of the pipe will give an equally large proportional error in  $\tau$  deduced from (38). This makes a flow law deduced from the upper parts of the pipe rather unreliable. We therefore reverse the procedure as follows.

Taking  $r = 0.14$  yr<sup>-1</sup>, and assuming the relation between  $\dot{\epsilon}$  and  $\tau$  given by Glen’s laboratory experiments, we deduce the dependence of  $\dot{\gamma}$  on  $\bar{\rho}g_x y$  from the equations

$$\dot{\gamma} = -2\sqrt{(\dot{\epsilon}^2 - r^2)}, \quad \bar{\rho}g_x y = \frac{\tau}{\dot{\epsilon}}\sqrt{(\dot{\epsilon}^2 - r^2)}. \tag{39}$$

Except for a surface layer of 15 m thickness which is penetrated by the winter cold wave, the whole of the Jungfrau firn at the altitude concerned is at the pressure melting-point (Hughes & Seligman 1939). Glen (1955) gives two flow laws for  $-0.02^\circ$  C, one referring to the quasi-viscous creep rate and the other to the minimum observed creep rate. We select the former, both on the general grounds that Glen discusses and because this curve shows the better agreement with the results from the contraction of glacier tunnels. Glen’s equation

$$\kappa = 0.017\sigma^{4.2}$$

for uniaxial compression becomes, in terms of  $\dot{\epsilon}$  and  $\tau$  (p. 486 of Nye 1953),

$$\dot{\epsilon} = \frac{\sqrt{3}}{2} \times 0.017(\sqrt{3}\tau)^{4.2} \quad \text{or} \quad \dot{\epsilon} = 0.148\tau^{4.2}$$

(strain rates in yr<sup>-1</sup>, stresses in bars). We then find the theoretical curve of  $\dot{\gamma}$  against  $\bar{\rho}g_x y$  shown in figure 6 as  $T_1$ .

Before comparing the theoretical curve with the result of the pipe experiment a complication in the interpretation of the experimental results must be mentioned. If the pipe were initially normal to the surface it would begin to tilt in proportion to the shear strain rate  $\dot{\gamma}$ . But, once tilted, the longitudinal extension rate  $r$  would produce a further tilt on its own account. The strain rate normal to the surface, assumed equal to  $-r$  (compressive), has the same effect. This means that the change of inclination of the pipe can no longer be straightforwardly interpreted as due to

shear strain alone. For a given depth, if  $\theta$  is the angle of inclination of the pipe to the surface normal ( $\tan \theta = dx/dy$ ), we have

$$\dot{\gamma} = \frac{d}{dt}(\tan \theta) - 2r \tan \theta.$$

Taking  $\dot{\gamma}$  to be constant and integrating we find

$$\dot{\gamma} = \frac{2r}{\exp(2rt_1) - 1} \{\tan \theta_1 - \exp(2rt_1) \tan \theta_0\}, \quad (40)$$

where  $\theta = \theta_0$  when  $t = 0$ , and  $\theta = \theta_1$  when  $t = t_1$ .

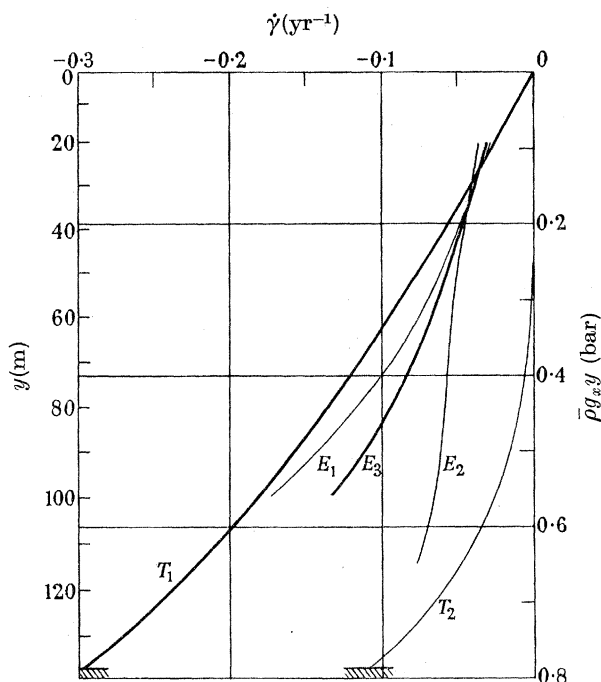


FIGURE 6. Rate of shear strain  $\dot{\gamma}$  as a function of shear stress  $\bar{\rho}g_x y$  in the Jungfrau firn.

$T_1$ , present theory ( $\alpha_1 = 4.0^\circ$ ,  $r = 0.14 \text{ yr}^{-1}$ );  $T_2$ , theory ignoring the longitudinal strain rate ( $r = 0$ ).  $E_1$ , experimental (15 August 1948 to 10 October 1949);  $E_2$ , experimental (10 October 1949 to 8 September 1950);  $E_3$ , best experimental curve (15 August 1948 to 8 September 1950).

The inclinations  $\phi$  measured in the experiment were to the vertical, and  $\phi$  and  $\theta$  are defined with opposite senses, so that  $\theta = -(\phi - \alpha_1)$ . As explained below  $\alpha_1$  is taken as  $4.0^\circ$ . From the measured values of  $\phi$ , I have calculated  $\theta$ , and hence  $\dot{\gamma}$  by equation (40). This has been done for various depths and for the periods 1948–49 (curve  $E_1$ ), 1949–50 (curve  $E_2$ ), and 1948–50 (curve  $E_3$ ). The values of  $\bar{\rho}g_x y$  used in plotting these experimental curves are smaller by a factor of 0.86 than the shear stresses calculated by Gerrard *et al.* because I have used a different value for the surface slope  $\alpha_1$ . Gerrard *et al.* took  $\alpha_1 = 4.6^\circ$ . This was calculated (private communication) from contour lines shown on a 1:25 000 map of the area, apparently

made in 1939 or earlier, and represents the average slope over a distance of 500 m. Kasser has measured the surface slope over a distance of 150 m, which is more nearly equal to the length of the pipe, by survey of the stakes referred to above, with the following results:

1946	1947	1948	1949	1950	1951	1952	1953	1954	1955
3.7°	4.1°	4.0°	3.8°	4.3°	3.6°	3.7°	3.7°	3.9°	3.9°

I have adopted the value 4.0°, which is the mean for the period 1948–50. The effect of taking a different value for the slope would be to change the vertical scale for the experimental curves in figure 6; a lower slope would raise them towards curve  $T_1$ .

An unexpected result of this analysis is that the experimental curves for the various periods no longer agree well with one another, whereas when interpreted by Gerrard *et al.* on the simple shearing hypothesis they agreed very well. The most reliable measurements are those made in 1948 and 1950; in 1948 the inclinometer was not well controlled in azimuth, but since the tube was nearly vertical this is not a serious defect; in 1950 the inclinometer worked well and gave reproducible results. In 1949, on the other hand, the inclinometer was not completely reliable, and below 100 m the values may be in error by as much as 5°. It seems therefore that  $E_3$  should be regarded as the best experimental curve.

The maximum difference between the shear rates given by curves  $E_3$  and  $T_1$  is  $0.048 \text{ yr}^{-1}$ , or  $2.8^\circ$  per year. It is difficult to estimate the maximum error of  $E_3$  in shear rate, but it is almost certainly less than this, and probably about  $0.6^\circ$  per year. Thus some discrepancy remains.

The most serious weakness of the present theory is that it ignores the drag of the valley sides, and so will overestimate  $\dot{\gamma}$ . This might account in full for the gap between  $T_1$  and  $E_3$ . Other possible sources of error are as follows:

(i) Plane strain has been assumed. There may well be a significant lateral strain rate, but its magnitude is unknown. This would not only affect the curve  $T_1$ , but, if compressive, as seems likely, would reduce the spread between the three experimental curves. If the magnitude of the lateral strain rate were known, there would be no difficulty in modifying the theory to allow for it.

(ii) Variations of strain rate in the  $x$  direction are not included in the theory, although they may be significant.

(iii) Errors in the measurement of the surface slope and of  $r$ .

(iv) Glen's flow law for ice has been used, whereas the upper layers of the glacier consist of firn. (A change of the constant in the flow law would give a change in vertical scale for curve  $T_1$ .)

(v) Kasser's surface measurements are assumed to be representative of the underlying layers of ice; effects due to creep of the firn have been ignored.

(vi) The ice is supposed not to move past the pipe, although it must slip along it. We must remember that a given element of ice changes its depth during the experiment, both because of the accumulation of new snow on the surface and because of the strain in the  $y$  direction. The shear stress acting on a given element of ice therefore changes. However, what is important from our point of view is not the

change of depth of an element of ice, but the change of depth of an element of the pipe (owing to slipping along the length of the pipe these are not the same). The latter change arises both from the accumulation of new snow on the surface and from the bending of the pipe. The error in the calculated shear stress from this cause may be about 0.03 bar (corresponding to 5 m of ice).

(vii) The weight of the winter snow produces an additional shear stress during the winter which we have neglected.

(viii) An error in the assumed density distribution would likewise lead to an error in the calculated shear stress.

The difference between the present theoretical result and the result given by the earlier theory which ignored the longitudinal strain rate is seen by comparing curves  $T_1$  and  $T_2$ .  $T_2$  is calculated for  $r = 0$  and gives values of  $\dot{\gamma}$  considerably smaller than those observed, particularly at small depths. The effect of including  $r$  is to increase the theoretical  $\dot{\gamma}$  at all depths. At a depth of 50 m the effect of ignoring  $r$  is to underestimate  $\dot{\gamma}$  by a factor of 50, while on the present theory  $\dot{\gamma}$  at this depth is overestimated by a factor of 1.33.

As the depth increases the effect of  $r$  becomes progressively less important (curve  $T_2$  approaches  $T_1$  as  $y \rightarrow \infty$ ), but in the Jungfraufirn  $r$  still makes an important contribution even in the deepest layers. In the upper layers, on the other hand, the longitudinal strain rate is the major part of the total strain rate. This has the interesting effect of making the curve  $T_1$  nearly linear at the top, for it is readily proved that in the uppermost layers, where  $r \gg \dot{\gamma}$ ,  $\dot{\gamma}$  is proportional to  $\bar{\rho}g_x y$  with an effective viscosity of  $2r/\tau^*$ , where  $r = f(\tau^*)$ . In other words, if the major part  $r$  of the strain in these layers is ignored, the minor part  $\dot{\gamma}$  behaves in an apparently viscous way, but with the coefficient of viscosity determined by  $r$ . To remove any misunderstanding let it be said at once that this fact gives no support at all to the constant viscosity theory of glacier flow.

Another interesting feature of the theoretical solution is the remarkable constancy of  $\tau$ ; it varies from 0.99 bar at the surface to 1.08 bars at the bed. This again is an effect arising from the dominant role of the longitudinal extension rate. It follows that in this particular place in the Jungfraufirn the approximation of perfect plasticity would be a good one. The depth of the Jungfraufirn is such that the lower parts of the perfectly plastic solution, where the strain rates are very large, and where the solution therefore breaks down for a real material, are never reached. The measured depth in fact corresponds to 0.72 of the critical depth of the perfectly plastic solution.

## REFERENCES

- Bauer, A. 1955 *Actualités Sci. Industr.* no. 1225. Expéditions Polaires Françaises. VI. Le Glacier de L'Eqe, pp. 86–8.
- Bull, C. 1957 Submitted to *J. Glaciol.*
- Gerrard, J. A. F., Perutz, M. F. & Roch, A. 1952 *Proc. Roy. Soc. A*, **213**, 546.
- Glen, J. W. 1955 *Proc. Roy. Soc. A*, **228**, 519.
- Hill, R. 1950 *The mathematical theory of plasticity*. Oxford: Clarendon Press.
- Hughes, T. P. & Seligman, G. 1939 *Mon. Not. R. Astr. Soc. Geophys. Suppl.* **4**, 616.
- McCall, J. G. 1952 *J. Glaciol.* **2**, 122.
- Nádai, A. 1931 *Plasticity*, pp. 221–226. New York: McGraw-Hill.
- Nye, J. F. 1951 *Proc. Roy. Soc. A*, **207**, 554.
- Nye, J. F. 1952*a* *J. Glaciol.* **2**, 82.
- Nye, J. F. 1952*b* *J. Glaciol.* **2**, 103.
- Nye, J. F. 1952*c* *Nature, Lond.*, **169**, 529.
- Nye, J. F. 1953 *Proc. Roy. Soc. A*, **219**, 477.
- Nye, J. F. 1955 *J. Glaciol.* **2**, 512.
- Orowan, E. 1949 *J. Glaciol.* **1**, 231.
- Orvig, S. 1953 *J. Glaciol.* **2**, 242.
- Perutz, M. F. 1954 *Proc. Roy. Instn. G.B.* **35**, 571.
- Prandtl, L. 1923 *Z. angew. Math. Mech.* **3**, 401.
- Robin, G. de Q. 1953 *J. Glaciol.* **2**, 205.
- Truesdell, C. 1950 *J. Math. pures appl.* **29**, 215.
- Truesdell, C. 1952 *J. Rat. Mech. Anal.* **1**, 225.
- Ward, W. H. 1955 *J. Glaciol.* **2**, 592.